Biomedical Optics EXPRESS

Real-time tissue differentiation based on optical emission spectroscopy for guided electrosurgical tumor resection

Dominik Spether,[1] Marcus Scharpf,[2] Jörg Hennenlotter,[3] Christian Schwentner,[3] Alexander Neugebauer,[4] Daniela Nüßle,[4] Klaus Fischer,[4] Hans Zappe,[1,*] Arnulf Stenzl,[3] Falko Fend,[2] Andreas Seifert,[1] and Markus Enderle[4]

[1]*Gisela and Erwin Sick Chair of Micro-optics, Department of Microsystems Engineering, University of Freiburg, 79110 Freiburg, Germany*
[2]*Institute of Pathology and Neuropathology, University Hospital Tuebingen,72076 Tuebingen, Germany*
[3]*Department of Urology, University Hospital Tuebingen, 72076 Tuebingen, Germany,*
[4]*ERBE Elektromedizin GmbH, 72072 Tuebingen, Germany*

[*]*zappe@imtek.uni-freiburg.de*

Abstract: Complete surgical removal of cancer tissue with effective preservation of healthy tissue is one of the most important challenges in modern oncology. We present a method for real-time, *in situ* differentiation of tissue based on optical emission spectroscopy (OES) performed during electrosurgery not requiring any biomarkers, additional light sources or other excitation processes. The analysis of the optical emission spectra, enables the differentiation of healthy and tumorous tissue. By using multi-class support vector machine (SVM) algorithms, distinguishing between tumor types also seems to be possible. Due to its fast reaction time (0.05*s*) the method can be used for real-time navigation helping the surgeon achieve complete resection. The system's easy realization has been proven by successful integration in a commercial electro surgical unit (ESU). In a first step the method was verified by using *ex vivo* tissue samples. The histological analysis confirmed, 95% of correctly classified tissue types.

OCIS codes: (170.6510) Spectroscopy, tissue diagnostics; (170.1610) Clinical applications; (170.3890) Medical optics instrumentation

References and links

1. Z. Huang, M. S. Bergholt, W. Zheng, K. Lin, K. Y. Ho, M. Teh, and K. G. Yeoh, "In vivo early diagnosis of gastric dysplasia using narrow-band image-guided Raman endoscopy." J. Biomed. Opt. **15**(3), 037017 (2010).
2. J. W. Spliethoff, D. J. Evers, H. M. Klomp, J. W. van Sandick, M. W. Wouters, R. Nachabe, G. W. Lucassen, B. H. W. Hendriks, J. Wesseling, and T. J. M. Ruers, "Improved identification of peripheral lung tumors by using diffuse reflectance and fluorescence spectroscopy." Lung Cancer **80**, 165–171 (2013).
3. J. Balog, L. Sasi-Szabó, J. Kinross, M. R. Lewis, L. J. Muirhead, K. Veselkov, R. Mirnezami, B. Dezső, L. Damjanovich, A. Darzi, J. K. Nicholson, and Z. Takáts, "Intraoperative tissue identification using rapid evaporative ionization mass spectrometry." Sci. Transl. Med. **5**, 194ra93 (2013).
4. N. Strittmatter, M. Rebec, E. A. Jones, O. Golf, A. Abdolrasouli, J. Balog, V. Behrends, K. A. Veselkov, and Z. Takáts, "Characterization and identification of clinically relevant microorganisms using rapid evaporative ionization mass spectrometry." Anal. Chem. **86**, 6555–6562 (2014).
5. B. Crawshaw and C. P. Delaney, "Gastrointestinal surgery: real-time tissue identification during surgery." Nat. Rev. Gastroenterol. Hepatol. **10**, 624–625 (2013).

#227055 - $15.00 USD Received 19 Nov 2014; revised 31 Jan 2015; accepted 31 Jan 2015; published 24 Mar 2015

6. A. Taheri, P. Mansoori, L. F. Sandoval, S. R. Feldman, D. Pearce, and P. M. Williford, "Electrosurgery: part I. Basics and principles." J. Am. Acad. Dermatol. **70**, 591.e1 (2014).
7. F. B. Calvo, D. Santos Junior, C. J. Rodrigues, F. J. Krug, J. T. Marumo, N. Schor, and M. H. Bellini, "Variation in the distribution of trace elements in renal cell carcinoma." Biol. Trace. Elem. Res. **130**, 107–113 (2009).
8. Z. Dobrowolski, T. Drewniak, W. Kwiatek, and P. Jakubik, "Trace Elements Distribution in Renal Cell Carcinoma Depending on Stage of Disease," Eur. Urol. **42**(5), 475–480 (2002).
9. A. S. Fassina, I. Calliari, A. Sangiorgio, M. Rossato, M. Ramigni, M. Dal Bianco, and F. Pagano, "Quantitative analysis of trace elements in human clear cell carcinoma of the kidney by energy-dispersive X-ray fluorescence," Eur. Urol. **18**(2), 140–144 (1990).
10. I. Steinwart and A. Christmann, *Support Vector Machines*, Information Science and Statistics (Springer, Springer Science+Business Media, 2008).
11. S. Keereweer, P. B. A. A. Van Driel, T. J. A. Snoeks, J. D. F. Kerrebijn, R. J. Baatenburg de Jong, A. L. Vahrmeijer, H. J. C. M. Sterenborg, and C. W. G. M. Löwik, "Optical image-guided cancer surgery: challenges and limitations." Clin. Cancer Res. **19**, 3745–3754 (2013).
12. D. Kamke and W. Walcher, *Physik für Mediziner* (Vieweg+Teubner Verlag, Wiesbaden, 1982).
13. W. D. Dupont and W. D. Plummer, "Power and sample size calculations for studies involving linear regression." Controlled Clin. Trials **19**, 589–601 (1998).
14. T. E. Oliphant, "Python for Scientific Computing," Comput. Sci. Eng. **9**, 10–20 (2007).
15. F. Pedregosa, G. Varoquaux, A. Gramfort, V. Michel, B. Thirion, O. Grisel, M. Blondel, P. Prettenhofer, R. Weiss, V. Dubourg, J. Vanderplas, A. Passos, D. Cournapeau, M. Brucher, M. Perrot, and E. Duchesnay, "Scikit-learn: Machine Learning in Python," JMLR **12**, 2825–2830 (2011).
16. S. van der Walt, S. C. Colbert, and G. Varoquaux, "The NumPy array: a structure for efficient numerical computation," Comput. Sci. Eng. **13**, 22–30 (2011).

1. Introduction

The gold standard for the treatment of many solid malignant tumors is complete resection. A general problem in surgical oncology is that the surgeon has the challenge to decide whether tissue is healthy (leave it in the patient) or malignant (cut and remove it from the patient). In the latter, the surgeon's interest is to conserve as much of the healthy tissue as possible for functional and cosmetic reasons. In case of doubt, the pathologist has to decide by histological evaluation of frozen sections intraoperatively. This takes usually 20 min and more. During this time the patient stays under general anesthesia and the surgical team has to wait for the diagnosis of the pathologist. Sometimes repeated tissue samples are even necessary. An improved surgical procedure which ensures that all malignant tissue is removed under real-time conditions is thus urgently needed.

Spectroscopic methods have a high potential for detection of cancer at an early stage. It has been shown that, for example, image-guided Raman spectroscopy can detect gastric dysplasia [1]; diffuse reflectance and fluorescence spectroscopy is able to detect peripheral lung cancer [2]; and evaporative ionization mass spectroscopy is capable of identifying various biological tissues [3–5]. None of these methods is in clinical use yet.

Electrosurgery has a wide range of applications in clinical practice, as for example in blood and tissue coagulation; vessel sealing (bipolar application); and cutting of tissue (monopolar application) [6]. The aim of the present study was to set up a novel methodology based on electrosurgical tissue dissection combined with an optical real-time diagnostic method to ensure that all malignant tissue is removed during surgery. To reach this aim, we developed a new kind of smart scalpel exploiting a by-product of electrosurgery, namely photons. In the following this new technology is described in detail.

2. Electrosurgical tissue identification system (electrosurgical OES-system)

At the moment of electrical activation, light, physically equivalent to a spark, which contains specific information about the target tissue is generated at the tip of the electroscalpel (Fig. 1). The electrosurgical system developed and described here (Fig. 2) uses the spark to enable real-time tissue analysis based on optical emission spectroscopy (OES). In the following, we use

#227055 - $15.00 USD Received 19 Nov 2014; revised 31 Jan 2015; accepted 31 Jan 2015; published 24 Mar 2015

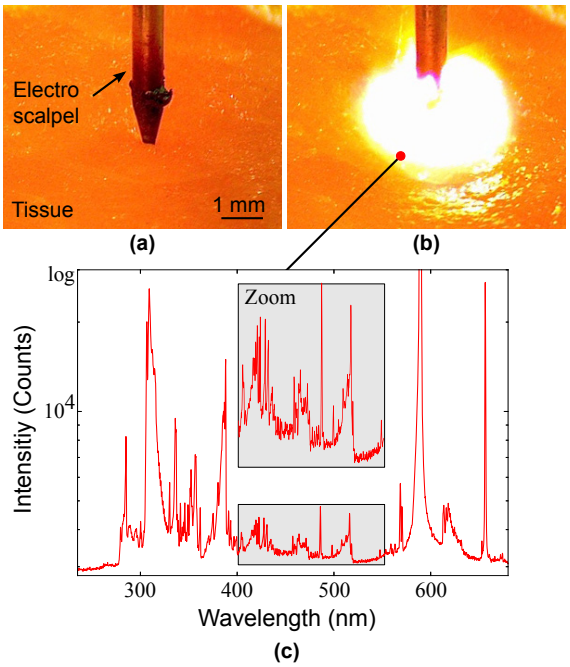

Fig. 1. (a) Microscope image of the tip of an electroscalpel and (b) light phenomenon appearing during activation. With an optical emission spectrometer, the spectral components of the spark are analyzed. (c) Typical tissue spectrum of the spark measured with our system. In the wavelength range of this example, bands and emission lines of atmospheric elements (N_2, O_2, H_2) and molecular fragments of biological molecules (proteins, DNA, ..), for example *NH*, *CH*, *CN* and *OH*, can be recognized. In addition, specific atomic emission lines of essential and trace elements as Ca, K, Mg, Na, P, Cl, Cd, Zn, Rb, Cr, Co, Fe, I, Cu, Mn, Mo, Se, F, Si, As, Ni, Sn and V are assigned in this range. The relative intensities of these emission lines depend on the concentrations of the elements. The combination of relative intensities of many peaks form a specific tissue finger print and allows real-time identification of tissue within milliseconds.

the terms *electrosurgical OES-system* for the entire apparatus and *OES-electroscalpel* for the handheld device. By activating the OES-electroscalpel, a spark develops between the tip of the monopolar active electrode and the tissue due to the high HF (high frequency) voltage applied. Tissue is vaporized instantaneously at the tip of the electrode as a result of a high current density and induced thermal effect. The molecules and atoms fragmented in this process are excited in the plasma of the spark to a higher energy level compared to their ground state. During relaxation back to the ground state, photons of specific wavelengths are then emitted. By means of optical fibers, the photons are captured at the distal end of the OES-electroscalpel and guided to an analysis unit which includes a conventional optical grating spectrometer with a spectral resolution of 0.5 nm and a spectral measurement range of 230 – 760 nm. Our OES-system reliably allows the identification of tissue by using an integration time in the range of 30 – 100 ms. The required integration time depends, for example on the design of the OES-electrode and the different types of tissue treated by the OES-scalpel. At the moment, we use an integration time of 30 – 50 ms for all tissue types (kidney, ...). To our knowledge, this setting is sufficient for all types of tissue differentiation we studied so far. To ensure a sufficient S/N -ratio, we perform the following two steps: First, we observe the intensity of the sodium D-line.

#227055 - $15.00 USD Received 19 Nov 2014; revised 31 Jan 2015; accepted 31 Jan 2015; published 24 Mar 2015

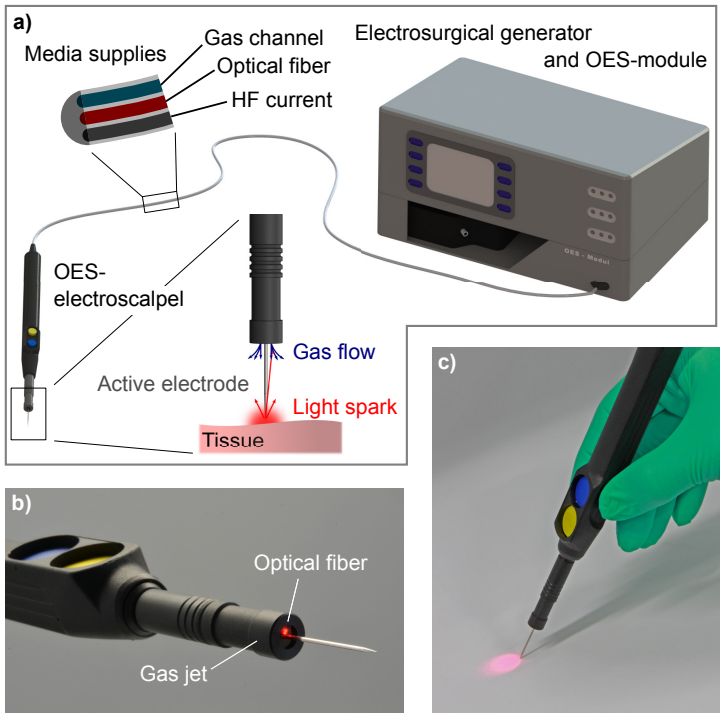

Fig. 2. Electrosurgical OES-system to perform high speed tissue identification. (a) Basic function of the system: Light of the generated spark is coupled into an optical fiber at the distal end of the electroscalpel. The fiber is protected against contamination by an argon gas stream during activation. By fiber optical technology, the photons are guided to an analysis unit consisting of a commercial optical grating spectrometer and a processing unit to allow real-time analysis of the tissue information in the spark. (b), (c) Prototypes of the OES-electroscalpel tested in a preclinical study. The functional optical fiber is visualized by red laser light coupled from the proximal side. All functional components required at an operating table are integrated into a standard electroscalpel.

After reaching a predefined threshold value, the spectral measurements of tissue are started. Second, we evaluate the intensity of the OH spectral band (306.3 nm), which we could identify in previous studies as a criterion to ensure sufficient signal-to-noise ratio. In the typical optical emission spectra of human tissue captured with this system (Fig. 1(c)), emission bands and lines of atmospheric elements (e.g. N_2) and molecular fragments can be seen. In addition, the specific atomic emission lines of essential and trace elements appear in this spectral range.

On a chemical level, the concentration of essential and trace elements like *Cd*, *Zn*, *K* and *Rb* differs in renal cell carcinoma tissue and healthy kidney tissue [7–9]. Deviations in the concentration of the elements lead to changes in relative intensity maxima of the emission lines in the spectrum. Additionally, the mechanical and electrical properties of the tissue have an influence on the produced plasma. This effect also leads to relative changes in the intensity of specific peaks. An algorithm we have developed uses the relative intensities of all the emission peaks in the spectrum as a characteristic tissue feature. Combining many such features yields a characteristic tissue finger print, and based on Support Vector Machines (SVM) [10], which are established algorithms for classification, tissue recognition is performed.

To realize a reliable tool for tissue differentiation, the algorithm first has to be trained

#227055 - $15.00 USD Received 19 Nov 2014; revised 31 Jan 2015; accepted 31 Jan 2015; published 24 Mar 2015

(Fig. 3(a)). A database consisting of the spectra of different tumors and healthy tissue is combined with the patient-specific tissue variances. For this, the surgeon takes spectra from healthy as well as tumorous tissue, which can easily be assigned and integrated into the database. After

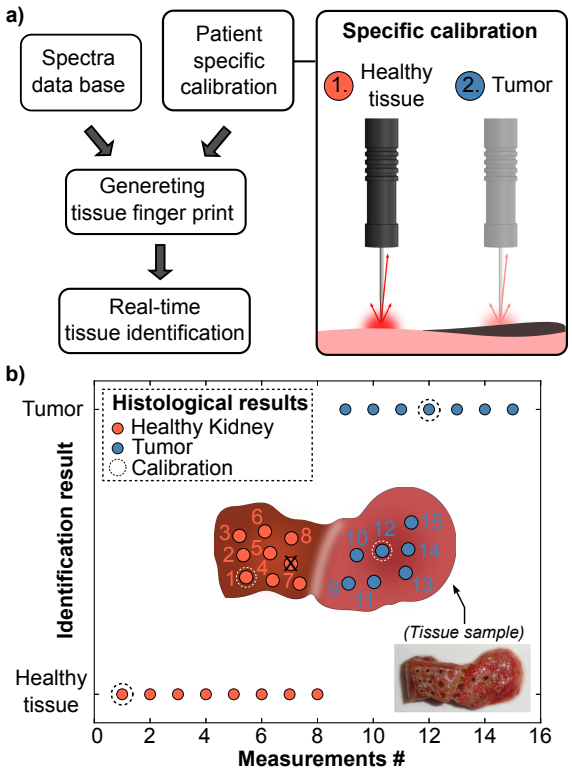

Fig. 3. Operational procedure of the OES-system. (a) The algorithm is first trained by including spectra from a patient-specific calibration into an existing database of spectra. In this way, the differentiation criteria (tissue finger print) can be calculated and real-time analysis is started. (b) Result of the tissue analysis with our system (y-axis) by means of a real tissue sample from the preclinical study (Section Preclinical pilot study, patient 11). Each point represents one measurement (x-axis); the color shows the histological result of each measurement point; the encircled points were used for calibration. In this example, all tissue measurements are correctly classified with our system. The point marked with an X is omitted, since no spectrometer data was available.

this patient-specific calibration, that normally takes $5-10$ seconds, real-time analysis can be started. The identification result (Fig. 3(b)) of a tissue sample from the preclinical study (Section *Preclinical study*) illustrates this procedure. The method allows identification of tissue within $30-50$ ms. This very quick analysis instantaneously provides the surgeon with the relevant information about the diagnosis of the underlying tissue during the cutting process (e.g. by warning visually using a blinking LED). With the help of this signal, the surgeon is able to both minimize the resection margin and to increase the potential of complete resection. This system has been integrated into a commercial electroscalpel and electrosurgical system.

#227055 - $15.00 USD Received 19 Nov 2014; revised 31 Jan 2015; accepted 31 Jan 2015; published 24 Mar 2015

3. Preclinical pilot study

3.1. Materials and methods

Study design

The non-inferiority study with the histology as gold standard served as study design. On the basis of Fisher's Exact Test with the statistical parameters $\alpha = 0.05$ (significance level), $statistical\ power = 0.8$ and a presumed accuracy rate of $P_0 = 0.98$ for the histology, the required number of samples for an accuracy rate with statistical significance (binary classification, tumor and healthy tissue) of $P_1 = 0.9$ is 161 tissue measurements. Since each measurement point was analyzed by histology the case group and the control group are independent and have the same size. In our statistical evaluation, we used the calculated sample size as test set size.

OES measurements

All tissue samples in the pre-clinical study have been extracted from nephrectomy specimens. Immediately after surgical resection, the specimens were cut from the organs by a pathologist at the University of Tuebingen and have been analyzed without any delay.

Histological analysis

Following the OES procedure, the specimens were fixed in formalin, embedded in paraffin and the prepared four-micrometer sections were stained with hematoxylin & eosin (Fig. 4). Each measurement point has been assigned to a histological result by the pathologist (M. S.).

Statistical evaluation

For planning the preclinical study and calculating the sample size, we used the software PS (Power and Sample Size Calculation) [13]. All statistical evaluations were performed with the programming language Python [14]. For this, the modules scikit-learn [15] and numpy [16] were mainly used.

3.2. Preclinical results

The system presented here was tested in a preclinical study to prove its reliability for tumor identification. Based on the hypothesis that we require a statistical significance of 90 % for the binary classification between healthy and tumorous tissue (see *Materials and Methods*), a minimum of 161 measurements is needed. We examined 229 tissue spectra from *ex vivo* samples of nephrectomy specimens, harvested within $10-30$ minutes after surgery, of 11 renal tumor patients. We chose the renal tumor because both tumorous and healthy tissue are resected to a sufficient extent; the difference between healthy and tumorous tissue is macroscopically quite obvious; and because renal tumors occur quite frequently. The trial had been accepted by the Institutional Review Board (IRB) of the University Hospital of Tuebingen (approval number 644/2011 B02). All patients gave their written consent for the study. The 11 samples comprised six Clear Cell Renal Cell Carcinoma (CCRCC), one Papillary Renal Cell Carcinoma (PRCC), one Chromophobe Renal Cell Carcinoma (ChRCC) and three Oncocytomas. All study samples contained both tumorous and healthy kidney tissue (Fig. 4). Each measurement point was examined by the OES-system and histology was performed by the Institute of Pathology and Neuropathology at the University of Tuebingen. These results served as a control group in the statistical evaluation.

Since the tissue identification algorithm uses all peaks in the tissue spectrum (Fig. 1(c)) to generate the differentiation criteria, the classification is done in a higher dimensional vector space. Each of these features (relative peak intensities) is equal to one dimension in this space. The resulting classification due to all of these criteria can thus not be plotted in two dimensions,

#227055 - $15.00 USD Received 19 Nov 2014; revised 31 Jan 2015; accepted 31 Jan 2015; published 24 Mar 2015

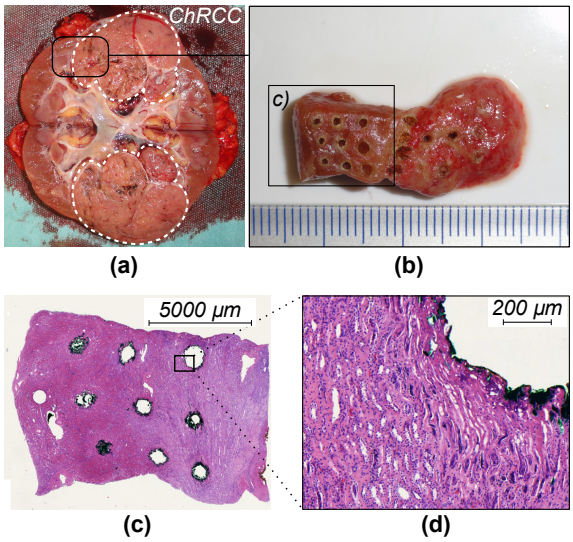

Fig. 4. Tissue sample from a preclinical study (Patient 11, ChRCC). (a) Nephrectomy specimen, (b) removed tissue sample, and (c,d) histological cut of the tissue sample after analysis with our system. Every lesion corresponds to one OES measurement. Each lesion was classified as tumorous or non-tumorous based on its histology.

yet to qualitatively visualize this mathematical methods from multivariant statistics, as for example linear discriminant analysis (LDA), have to be applied. This procedure allows one to reduce the dimensions down to $n-1$ ($LD_1, LD_2, \ldots, LD_{n-1}$), where n is the number of different tissue groups. Each point in the illustrated result of the LDA (Fig. 5), corresponds to a tissue

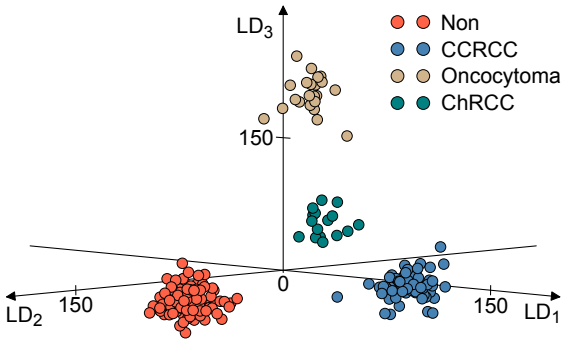

Fig. 5. Results of the Linear Discriminant Analysis. Each point corresponds to one OES measurement; the color encodes the histological result of the measurement. The red points, for example, represent the measurements of healthy tissue, whereas blue points indicate the identification of CCRCC. This analysis illustrates, that it is possible to differentiate between healthy tissue (red) and tumorous tissue. Moreover, different types of tumors can also be classified. The purpose of this plot is to qualitatively illustrate the reliability in tissue differentiation. Because of small sample size (two measurements) the PRCC measurements are not considered in this plot.

analysis with the OES-system. The color of the points symbolizes the histological result of the

#227055 - $15.00 USD Received 19 Nov 2014; revised 31 Jan 2015; accepted 31 Jan 2015; published 24 Mar 2015

measurement point. As the variance within the tissue groups (healthy tissue, CCRCC, Oncocytoma, ChRCC) is smaller than the variance between different tissue groups, it is possible to distinguish between healthy and tumorous tissue (binary classification). Moreover, the method also seems to allow classification of different tumor types.

To receive a first estimate of the reliability of tumor classification with the OES-system, the preclinical measurements were analyzed with different statistical methods (Table 1). In

Table 1. Results of the clinical trial with the OES-system. All OES measurements with successfully performed histological analysis have been evaluated ($N = 229$). The leave-one-out cross-validation was carried out for each individual patient as well as for the whole dataset. A shuffle-split cross-validation approach was applied to the whole dataset.

Patient	Tumor type	n spectra	Sensitivity	Specificity	Positive Predictive Value	Negative Predictive Value	Accuracy rate
			Leave-one-out cross-validation				
1	Oncocytoma	13	1.0	0.857	0.857	1.0	0.923
2	Oncocytoma	13	0.833	0.857	0.833	0.857	0.846
3	PRCC	5	1.0	1.0	1.0	1.0	1.0
4	Oncocytoma	17	0.900	1.0	1.0	0.875	0.941
5	CCRCC	11	1.0	0.833	0.833	1.0	0.909
6	CCRCC	25	1.0	1.0	1.0	1.0	1.0
7	CCRCC	12	1.0	0.750	0.889	1.0	0.917
8	CCRCC	32	0.917	1.0	1.0	0.952	0.969
9	CCRCC	25	1.0	1.0	1.0	1.0	1.0
10	CCRCC	44	1.0	0.950	0.960	1.0	0.977
11	ChRCC	32	0.938	1.0	1.0	0.941	0.969
							Correctly classified tumor type
All Patients		229	0.982	0.956	0.958	0.982	0.956
			Shuffle-split cross-validation				
All Patients		229	0.930	0.929	0.932	0.929	0.929
Mean values			**0.96**	**0.93**	**0.94**	**0.96**	

the shuffle-split cross-validation, a random sample consisting of 30 % of the spectra recorded in the study ($N = 68$) is taken to train the system. With the remaining number of $N = 161$ measurements, tissue identification is carried out and the result is compared with the histological analysis. The random split approach is repeated in a loop 100,000 times. The calculated values from each iteration of specificity, sensitivity, Positive Predicted Value (PPV), Negative Predicted Value (NPV) as well as the correctly classified rate were averaged and summed in the table. The first four values describe the reliability of differentiating between tumorous and healthy tissue, whereas the last value shows the fraction of correctly identified tumor types.

In addition to this, a leave-one-out cross-validation was performed for each individual patient as well as for the entire dataset. In this standard method, $n-1$ out of n spectra are used as training sets. Subsequently, the remaining spectrum is classified by comparing it with the histological result. The final result after all evaluations greatly substantiates the reliability of

#227055 - $15.00 USD Received 19 Nov 2014; revised 31 Jan 2015; accepted 31 Jan 2015; published 24 Mar 2015

the developed method by the following mean values:

$Sensitivity = 0.96$, $Specificity = 0.93$, $PPV = 0.94$, $NPV = 0.96$.

Beyond this, an average of 95 % of correctly classified tumor types was identified with these measurements.

4. Discussion

A number of different technologies, such as optical image-guided cancer surgery, are currently under investigation to achieve *in situ* diagnostics of the resection margins without additional frozen sections [11]. A completely new procedure is the *Intelligent Knife*, that vaporizes tissue using electrosurgery, and the smoke by-product is analyzed by means of mass spectroscopy [3–5]. The smoke is sucked away through a flexible tube, with a standard length in electrosurgery of $2-4$ m, into the mass spectrometer. The corresponding time for reliably analyzing tissue thus takes $0.7-5$ s [3,4] and thus does not allow real-time analysis. With this approach, guided surgery that yields complete removal of the tumor but keeps the resection margin as small as possible is only possible to a limited extent. In contrast to smoke analysis by mass spectroscopy, the spectroscopic analysis of the spark and SVM based tissue classification is done in 50ms by using the OES-System.

In the OES-system described here, a signal (for example a blinking LED) can be used to warn the surgeon if the cutting electrode unintentionally moves into the tumor tissue. This information allows the surgeon to effectively resect tumorous tissue. Assuming an average human reaction time of 210 ms [12] and a cutting velocity of $4\,\frac{\text{mm}}{\text{s}}$, a theoretical spatial resolution of 0.8 mm is expected for our system. The active electrodes in surgical use have an average diameter of $0.6-0.8$ mm, hence the width of the resection margins can conceivably be reduced to below 1 mm.

A particular strength of the OES approach, in contrast to other methods, is that the identification of tissue can be accomplished without the need for any biomarkers. Another advantage is that no additional light source or other means for excitation is required; the HF method by itself delivers the diagnostic information. Furthermore, the tissue calibration described above offers the potential for a patient-specific differentiation of tumor and tissue types which do not yet exist in the current database.

High-tech diagnostic procedures often need big, expensive and maintenance-intensive physical instruments, such as the mass spectrometer in the *Intelligent Knife* system. Since standard devices from optical emission spectroscopy (e.g. the small-footprint optical grating spectrometer) and electrosurgery are well established, costs can be reduced to a minimum. To extend the capabilities for tumor identification, the OES-system can be combined with known tissue identification systems and methods, such as microscopical procedures, smoke analysis or medical imaging technology as CT or MRT. Because of these findings the OES-system offers a great potential for realizing real-time guided tumor resection.

Limitations of our work are that the data represents only preclinical data, only renal tumor and small number of cases. Renal tumors are usually entirely encapsulated and thus the tissue boundaries are clearly defined. There are many other tumors with undefined tissue boundaries. Therefore, these findings need to be confirmed for other tumor types and as a next critical step a prospective clinical study needs to be performed.

5. Conclusion

The developed OES tissue identification system thus fulfills the demand for fast reaction time and allows the integration of all measurement components to be used at an operating table into a standard electroscalpel. First experiments demonstrate its suitability for real-time analysis of tissue composition during tumor resection according to very promising preclinical results

#227055 - $15.00 USD Received 19 Nov 2014; revised 31 Jan 2015; accepted 31 Jan 2015; published 24 Mar 2015

(sensitivity, specificity, NPV, PPV greater than 90 %).

Acknowledgment

We thank Clemens Wachter for his assistance in the English translation.

#227055 - $15.00 USD Received 19 Nov 2014; revised 31 Jan 2015; accepted 31 Jan 2015; published 24 Mar 2015